Thermodynamics of Philicphobic Interaction Shift in Aqueous Tweens 20-80

Man Singh*, Jainita S. Patel, R. K. Kale

School of Chemical Sciences, Central University of Gujarat, Gandhinagar
Gujarat 382030, India
Email:*mansingh50@hotmail.com, jainitapatel@ymail.com, raosahebkale@gmail.com

Abstract

Density ($\rho \pm 10^{-3}$ kg m^{-3}), surface tension ($\gamma \pm 10^{-2}$ mNm^{-1}) for 8.4 to 83.6 mmol kg^{-1}(mmk) at 8 mmk intervals aqueous polyoxyethylene sorbitan monolaurate (C=12, Tw20), monopalmitate (C=16, Tw40), monostearate (C=18, Tw60) and monooleate (C=18, 1 double bond, Tw80) nonionic surfactants at 293.15 K are reported. Apparent molar volumes (V_2) are derived from densities. The γ is used for surface excess tension (γ^{excess}, mNm^{-1}), concentration (τ, mol m^{-2}) and area per molecule (a=1/τ, m^{2}mol^{-1}). The ρ and γ were regressed for limiting ρ^0 and γ^0 respectively and slopes for a shift from hydrophilic to hydrophobic interactions. The $\rho^0_{Tw20} > \rho^0_{Tw40} > \rho^0_{Tw80} > \rho^0_{Tw60}$ and $V_2{}^0_{Tw60} > V_2{}^0_{Tw40} > V_2{}^0_{Tw80} > V_2{}^0_{Tw20}$, the limiting densities and apparent molar volumes respectively in opposite order, have inferred stronger structural interaction with Tw20 and weaker with Tw60. The $\gamma_{water} > \gamma^0_{Tw80} > \gamma^0_{Tw40} > \gamma^0_{Tw20} > \gamma^0_{Tw60}$ inferred as 18% weakening of their cohesive force in comparison to water, especially, the Tw60 has caused a 22.68% decrease in the cohesive force. These variations in the γ^0 data along with their slope have revealed different interacting chemical potentials (μ, J m^{-2}) and entropic change (ΔS, J mol^{-1}K^{-1}). The MPK model is proposed to illustrate the critical impact of the hydrophilic-hydrophobic actions depicted as μ^S and μ^B with $\mu^B < 0 < \mu^S$ thermodynamic state. The μ^S and μ^B are interacting chemical potentials of surface and bulk phases respectively.

Keywords: Intermolecular forces; density; excess surface tension; area per molecule; chemical potential; entropy; Tweens; micelles; molar volume.

1. Introduction

Tweens (Tw) as nonionic surfactants (NIS) are constituted of polyoxyethylene sorbitan (POES) [-(-OCH$_2$CH$_2$)$_5$OH]$_4$C$_4$H$_5$O] and fatty acids as hydrophilic and hydrophobic parts respectively with individual interacting activities. Each part has a specific electronic configuration with different actions due to molecular constitutional force (MCF) which is directly related to FTIR in stretching frequencies. The individual part has specific constituents with specific covalent bonding force (CBF) which is not only in case of ionic systems but also with Tw where the CBF responds to FTIR as integrated molecular unit. Had the CBF and MCF not been in the molecule, then the same would not have behaved as a molecular unit. Thus the CBF and MCF are the binding tools where each and every unit has a different MCF and CBF to induce interactions. The CBF is a part of MCF via covalent bonds between two atoms attached in an alkyl chain (AC). If these two forces are so strong and not disrupted by solvents then individual parts maintain their identity. However the Tw interacts and if reacting then is noted as a remarkable model for interactions which may be extended to organic reactions. But when the forces are weaker and overcome by the solvent on mixing then the systems are noted as thermodynamically active due to transformational chemical changes. Thus, the Tw interactions are fitted in these models to depict their thermodynamic activities. If the MCF and CBF are not influenced by interactions and remain in their original form except for minor twisting then their orientation works based on permanent dipoles. It is monitored by a concept of Maxwell-Wagner-Sillars

polarization (Denial et al, 2003; Kohler et al, 2008) with charge separation in dielectric electrostatics. The MCF and CBF induce weaker activities with minor thermodynamic changes. So their mixtures are non-reactive and interactive as is depicted with various physicochemical indicators (PCI) such as density and surface tension. The above mentioned argument distinguishes between the reacting and interacting systems. Therefore aqueous Tw solutions are highly thermodynamic and their philicphobic interacting (PPI) mixtures are in high demand as a potential medium for analysis of interacting activities and mechanisms. The Tw constitutes aqueous non-ideal mixtures with thermodynamic excess properties (Lee et al, 2005). With exceptionally higher chemical potentials, the Tw induces binding and hydrogen bond (HB) disruption capacities to design liquids with specific properties. Thus, their study becomes necessary for industrial and academic uses (Singh et al, 2010a). Sorbitan as a monoester of fatty acids with 3 free polyethyleneglycole (PEG) units is reported as polysorbates or Tw.

The Tw incorporates covalent bonding, van der Waals force, London dispersive, Lennard Jones potential and Lorenz force which are often used as approximate models for molecular activities such as repulsion and attraction (Denial et al, 2003). Several constitutional factors such as polarization, orientation of atomic oscillations or electronegativity in a localized area on a pattern of Linear combination of molecular orbital (LCMO) with covalent bonds could have an impact on IMF as a key for interacting potential. Thus dielectric polarization and charge separation influence polarization density, volume dielectric

polarization and potential gradient or vacancy of equilibrium potential with molecular activities. The Tw sustains sorbitan, PEG and fatty acids which interact differently with aprotic dipolar or protic polar solvents due to having specific MCF and CBF. The aprotic dipolar solvents such as water do have Columbic attractions while on the other hand the Tw as highly viscous induces Lennard Jones potential and London dispersive forces where a gradient is developed as a driving force for interactions. Many dimensions and interacting models are used to solve or characterize molecular mixtures with n number of constituents. For example, the constitutional characteristics of sorbitan esters induce emulsifying activities in creams and ointments for pharmaceutical, cosmetic, food processing as wetting agents, suspensions in medical use, detergents, biotechnology and domestic applications. In such applications our data could render useful help for understanding interacting patterns. It could depict theoretical and mathematical correlations within interacting variables for interfacing the integrated and differentiated driving forces being functional in CBF and Columbic force (Figure 1) respectively. The Tw tend to low surface energy liquids with structural occurrence and spreading forces among 3 PEG units due to Lennard Jones potential associated with respective units.
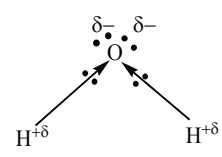
$$F = k\left(\frac{q_+ q_-}{r^2}\right) \quad \text{For dipolar water}$$

Figure 1. The q_+ and q_- are point charges at r distances from dipolar water.

The point charges (Figure 1) are missing in the Tw due to charges spreading along with their hydrophilic and hydrophobic domains. The system is thermodynamically fascinating and challenging as several interacting forces do operate. Of course, a wider study is reported on Lennard dispersive, Lorenz and Columbic forces but a science is still needed to extend to wider applications. The Tw causes critical and optimized configurational structures within IMF operating for mixing with longer AC with CBF, and critical structural interactions may not occur and could form a cage around AC (Bakshi et al, 2006; Singh, 2008). The solvent energy is used to activate Tw with molecular oscillations in vibrational mode around a central point of equilibrium between hydrophilic and hydrophobic domains (Singh & Sharma, 2006a; Valery et al, 2008) with vibration energy $E_v = (v+1/2)\ hv^0$. It might negligibly contribute to a dynamical interaction shift with v = 0, 1, 2, n as the vibration quantum number for energy (E_{mol}). For Tw mixing, the E_{mol} is constituted of electronic, vibrational, rotational, nuclear, and translational components with many degrees of freedom as follows.

$$E_{mol} = E_{electronics} + E_{vibrational} + E_{rotational} + E_{nuclear} + E_{translational} \quad (1)$$

Eq. (1) integrates and differentiates constitutional factors for reorientational interaction with $E_{electronic}$ or potential energy for geometrical and oscillatory equilibrium. The atoms and ions cause interatomic forces due to consistent vibrations away from equilibrium with electrostatic charges (Hafner, 2003).

The Born-Oppenheimer Approximation explains electronic and nuclear simulations to generate frequencies for atomic vibrations of 10^{13} Hz and with 10^{-11} m amplitude (Elliott et al, 2006) in –C-C- in case of CBF. The atomic vibrations, covalent, ionic, semiconductors and interstitial phase (Dubost, 1998) could influence structural approximations with sp^3 hybridization. Both the induction and steric effects operate on AC and hybridization partly could contribute to cage formation. The philicphobic induced distribution and diversified forces depicted with ρ, γ magnitude as PCI which elucidate a structural shift. The PCI in context of intrinsic or orbital energy level of sp^3 and sp^2 molecular orbital and electrostatic interaction around a nucleus could be as $E_n = -hcRZ^2/n^2$, where R is Rydberg constant, Z is atomic number, n is the principle quantum number, h is Plank's constant, and c is speed of light. Thus a shift in shared electron pair induces (Rossnagel & Smith, 2006; Bartschat, 1992; Singh et al, 2010b) hydrophilic interactions within 10 to 20 nm configuration and influences hydrogen bonds (HB) (Jianbin et al, 2008; Wendlandt, 2005). The hydrophilic interaction could influence the ρ and γ data which directly mark structural changes.

2. Materials and method

Tw (98.99% s. d. fine-CHEM, Mumbai, India) were used as received, mixtures were prepared, w/w, with Milli-Q water (Millipore Integral 3) at similar experimental conditions. The pH 7 was maintained and checked with a standard method. The ± 0.01mg KERN (AVON Corporation LTD) balance was used for weighing. The Tw were kept for 2 - 4 h for solubilisation while smoothly stirred with Borosil glass rod at 40 rpm to avoid froth formation. The ρ was measured with Advanced Density and Sound Velocity meter (DSA 5000M, Anton Paar) by filling 3 mL in DSA Quartz U tube within 20 s for a sample and 80 s for pure Tw at ± 0.01^0C. The DSA 5000 M was calibrated with Milli-Q water and air. For each data the tube was cleaned by passing water and air until it was absolutely cleaned to avoid contamination while γ was measured with Survismeter, catalogue no. 3453 (Borosil, India), calibration no. 06070582/1.01/c-0395, NPL, New Delhi (8) (12, 13). The Borosil mansingh Survismeter was calibrated freshly with Milli-Q water with pendant drop numbers (n) (Singh, 2005). The measurements were error proof with high reliability data whose statistical analysis showed 95.5% confidence variance. The measurements were repeated several times for reproducibility, accuracy and precision at ± 0.05 °C temperature control.

2.1. Contact angle theta (θ) correction

Scientifically the pdn are formed when a specific weight (mg) of individual drop accumulated at a lower circumference of capillary of specific id (r, mm) becomes equal to the γ, depicted with Eq. (2).

$$mg = \pi r \gamma \text{Sin}\theta \quad (2)$$

The m is mass of a drop, g is gravitational force (9.81 ms^{-2}), r is capillary id and θ is contact angle in degrees. In general, a falling pdn around a capillary circumference forms a contact angle θ < 90^0. A tip of capillary was sharpened that formed a contact angle θ = 90^0 where sin (90^0) = 1. The sin(90^0) = 1 is kept in Eq. (2) for Eq. (3).

$$mg = \pi r \gamma \qquad (3)$$

It has assisted pdn formation for calculation of the γ with their fixed buoyancies.

3. Results and discussion
The ρ was regressed with Eq. (4).

$$\rho = \rho^0 + S_\rho m + S_\rho {}' m^2 \qquad (4)$$

The ρ^0 at m $\rightarrow$0 is the limiting density, and the S_ρ is 1st and S_ρ' 2nd degree slopes. Apparent molar volume (V_2) was calculated with Eq. (5).

$$V_2 = \frac{M}{\rho} - \frac{1000(\rho - \rho^0)}{m\rho\rho_0} \qquad (5)$$

M is molar mass, m is molality, and the ρ^0 and ρ are densities of solvent and mixture respectively. The V_2 are fitted in Eq. (6) (Singh & Kumar, 2006b; Singh & Sharma, 2006a Singh & Sushama, 2009).

$$V_2 = V_2^0 + S_v m + S_v {}' m^2 \qquad (6)$$

Surface tension (γ) was calculated with measured pendent drop numbers (n) data as Eq. (7).

$$\gamma = \left(\frac{n^0}{n} \right) \left(\frac{\rho}{\rho^0} \right) \gamma^0 \qquad (7)$$

The γ^0 is solvent surface tension. The n^0 and n are pendent drop numbers of solvent and mixtures respectively. The γ was regressed for limiting γ^0 at m $\rightarrow$0 and the slope (S_γ) values with Eq. (8).

$$\gamma = \gamma^0 + S_\gamma m + S_\gamma {}' m^2 \qquad (8)$$

The τ is surface excess concentration and was derived with the Josiah Willard Gibbs Eq. (9).

$$\tau = -\frac{1}{RT} \left(\frac{\partial \gamma}{\partial \ln c} \right) \qquad (9)$$

The c is concentration in bulk, R is the gas constant, and T is temperature. The τ is positive and inferred from the correlation between concentration and γ of Tw (Singh & Mutsuoka, 2009). Excess surface tension (mNm^{-1}) and area per molecule (m^{2}mol^{-1}) at surface are fitted with Eqs. (10) and (11) (Mitropoulos, 2008).

$$a = \frac{1 \times 10^{20}}{N\tau} \qquad (10)$$

The N is Avogadro number.

$$\gamma^{excess} = \gamma_{ref} - \gamma^0{}_{mixture} \qquad (11)$$

The γ_{ref} and $\gamma_{mixtures}$ are the surface tensions of water as a reference and of the mixture respectively. The surfactants have different concentration in the bulk (c, mol kg^{-1}) and at the interface (τ, mol m^{-2}) due to hydrophilic and hydrophobic interactions (HH$_b$I) respectively. The surface (μ^S) and bulk chemical potential (μ^B) were calculated with Eqs. (12) and (13).

$$\mu^S = \mu^0 + RT \ln c_S \qquad (12)$$

$$\mu^B = \mu^0 + RT \ln c_{bulk} \qquad (13)$$

The c_S and c_{bulk} are concentrations at the surface and in the bulk respectively. The entropy is calculated with Eq. (14).

$$\Delta S = R \ln \left(\frac{\gamma V}{h N_A} \right) \qquad (14)$$

Here R= 8.314 J ml^{-1}K^{-1}, T= 293.15 K, h = 6.62 $\times$ 10^{-34} m^2 kg / s and N_A= 6.023 $\times10^{23}$ mol^{-1} and are defined as follows: R (gas constant); h (Plank constant); N_A (Avogadro's number); V (AMV); and, γ (surface tension). The Tw with dipolar water developed structural interactions due to intermolecular forces (IMF) in the form of CBF and MCF. Before mixing, the free energies (ΔG) are as $\Delta G_{Tw} \neq \Delta G_{water}$ due to individual constitution but on mixing the ΔG is as $\Delta G_{Tw} = \Delta G_{water}$. The ΔG_{Tw} and ΔG_{water} belong to Tw and water respectively. The sample mole fractions were constant and dn_1 and dn_2 were equal to zero and ΔG_{mix} is denoted with Eq. (15).

$$dG_{mix} = \left(\frac{\partial G}{\partial T} \right)_{p,n1,n2} dT \qquad (15)$$

At fixed temperature, the interactions are a function of mole fractions and denoted with Eq. (16).

$$dG_{mix} = \left(\frac{\partial G}{\partial n_1} \right)_{T,P,n2} dn_1 + \left(\frac{\partial G}{\partial n_2} \right)_{T,P,n1} dn_2 \qquad (16)$$

In mixing, the ΔG_{mix} substantially decrease as $\Delta G_{mix} < 0$ with a spontaneous process due to chemical work done in dissolution and the energy was utilized. The equation $q = \Delta E + P\Delta V$ as the 1st law of thermodynamics explains the energy utilization. The q is unused energy in calories or Joules, and ΔE is the change in internal energy of Tw and water for the interaction. The P is the internal pressure exerted by IMF associated with interacting Tw and the ΔV is the resultant volume due to interactions. Thus the $\Delta G_{(Tw + water)} < 0$ inferred occurrence of philicphobic interaction (PPI) means the negative value of ΔG inferred the interaction due to Tw, POES as hydrophilic and fatty acids as hydrophobic domains respectively (Singh, 2006a). The PCI elucidated internal rearrangements and alignments in geometries with HB disruption in bulk or hydrogen bonded water (HBW) induces caging around hydrophobic AC at the surface as a significant criteria (Singh, 2006b). Thus the PCI analyzed effective and workable information for categorizing and looking for useful sciences of physicochemical functions (PCF).

3.1. Density
The Tw developed structural interactions due to IMF and MCF having definite values of ρ and γ. It analyzed

Table 1. The data of pure Tweens.

Functions	Tween 20	Tween 40	Tween 60	Tween80	Water
Density, 10^{-3}kg m^{-3}	1.105328	1.080207	1.082909	1.077190	0.998205
Surface tension, mN/m	46.37	43.78	46.87	43.84	72.88

internal pressure reflected as $\rho_{Tw20} > \rho_{Tw60} > \rho_{Tw40} > \rho_{Tw80} > \rho_{H2O}$, with stronger IMF than water (Table 1), especially, the Tw20 with 10.73% higher density. The Tw developed almost 11 times stronger interactions as compared to water. The Tw20 of C=12 with structural constituents of POES (Figure 2) caused interactions as hydrophilic > hydrophobic (Table 1). Densities decreased by 0.02512×10^3 kg m^{-3} on increment in C by 4C of the Tw40 and POES were unchanged. So a lowering is attributed to weakening of hydrophilic and strengthening of hydrophobic interactions (H$_b$I) in the same proportion. It is termed as a shift in interacting dynamics (ID) from hydrophilic to hydrophobic parts with micelles formation (Figure 2). An increment in AC from Tw20 to Tw60 is by 6 C with 0.02242×10^3 kg m^{-3} decrease which is lower as compared to Tw40. It may be because of comparatively longer AC than that of the Tw40. The latter has almost equal size of POES and AC with equilibrated shift in ID and increment in AC from Tw20 to Tw80 by 6C decreased density by 0.02814×10^3 kg m^{-3}. It has elucidated a role of double bond (DB) in oleic acid of Tw80. Thus in general, increments in AC weakened hydrophilic and strengthened hydrophobic where the DB also strengthened HI.

Because in Tw80 the DB is at 10th position C in AC and the Tw80 have 18C AC so remaining 8C acts hydrophobically. The hydrophilic rich Tw20 showed maximum density and the Tw80 minimum with stronger IMF due to stronger hydrophilic interactions (HI). Hence the hydrophobic AC developed weaker IMF with lower densities due to the water repelling nature toward hydrophobic AC while the higher IMF inferred that 3 ethylene glycol units (EGU) with free -OH groups developed at least 3 times higher IMF than of the water (Figure 2). The hydrophilic part developed stronger IMF than the hydrophobic with higher ρ. For example, the hydrophilic domain of the Tw20 dominated over the H$_b$I. A sequential expression of the ρ_{pure} must be $\rho_{Tw20} > \rho_{Tw40} > \rho_{Tw60} > \rho_{Tw80}$ with weaker hydrophilic and stronger H$_b$I with increment of C in AC. Probably the philicphobic strengths of EGU and AC become equal and the Tw60 becomes aggregated as no disbalancing forces exist in either hydrophilic or hydrophobic (Singh, 2006a; Kao et al, 2005). Hence no additional driving force exists where aggregated structures developed stronger packing geometries. The solvent has equally entered or is bounded with philicphobic components and the Tw60 remained suspended without getting settled. The water binding capacity of hydrophilic and cage formation capacity of hydrophobic parts are equal in Tw60.

The situation becomes like a Schrodinger equation with well-defined energy well within boundaries of hydration spheres of philicphobic areas with zero potential difference. The Tw40 and Tw80 produced lower densities with weaker IMF due to longer AC with weaker hydrophilic but stronger H$_b$I.

3.2. Binary systems

The Tw caused stronger IMF due to having advanced hydrophilic units, and developed a stronger network with higher intramolecular forces. When Tw is added in water, it disrupts HB between pure molecules that decreased ρ relative to a pure molecule and increased ρ relative to water (Table 2). The ρ increased with an increase in compactness and molecular mass with $\rho^0_{Tw20} > \rho^0_{Tw40} > \rho^0_{Tw80} > \rho^0_{Tw60}$ (Table 3). Hence the Tw60 produced the lowest ρ^0 with stronger H$_b$I and weaker HI. The Tw80 with DB has slightly weakened H$_b$I by compensating the HI. Thus the Tw80 developed a slightly lower IMF. It has explained the dynamic shift of hydrophilic to hydrophobic interacting activities (IA) and a role of Tw80 DB. It has distinguished the Tw20 and Tw80 because a Tw20 has weaker H$_b$I and stronger HI than those of the other. So an additional attachment of AC in Tw40, Tw60 and Tw80 of 4, 6 and 6 C (1 DB) respectively is operational and distinguished. The IMF and molecular activity (MA) justified lower densities of the Tw60 as its interacting strength where the molecules are configured with C-C chain and POES with H$_b$I and HI respectively. Comparatively the higher densities with Tw20 and lower with the Tw80 are due to stronger IMF with stronger HI (Tables 1, 2). It is fitted in proposed model of HI and H$_b$I where a shorter AC of Tw20 developed weaker H$_b$I while the POES developed the stronger HI. It is also applicable to Tw40, Tw60 and Tw80 with larger AC. The H$_b$I with Tw80, Tw60 and Tw40 dominates over HI and the philicphobic are efficiently operational and extendable to similar others with an increment in IMF with the same rate. The ρ could be an indication to visualize and interpret structural reorientation and molecular activities where the $S\rho_{Tw20} > S\rho_{Tw60} > S\rho_{Tw40} > S\rho_{Tw80}$ slopes inferred hydrophilic > hydrophobic due to the interacting activity of Tw with stronger compositional effects of the Tw20 (Table 3). Hence the Tw80 showed the lowest $S\rho_{Tw80}$ value as the HI is subjugated by H$_b$I with weaker compositional impact with mild ID and weaker participation in solute solvent interaction.

The slopes of Tw60 are slightly lower than of the Tw20 with 18 AC (steric hindrance). The C18 (AC) + 10 C (EG) {tail} = 28 C chain in effect while the 3 EGU each with free -OH partly developed PPI. Each EGU is made up of 5 EG where a hydrophobic effect is moderate in comparison to the hydrophilic effect of each -OH. The EGU with 10 C + 30 C are under the influence of free -OH with hydrophilic IA. The AC and -OH developed philicphobic networking with a gel formation which seems to be slighter more active than those of the Tw40. However, the Tw40 has similar networking of hydrophilic units but AC with hydrophobic is lower with weaker activity level as compared to lower slope density.

The V_2 decreased with increase in molalities and is fitted in a concept of "the stronger the IMF and higher the internal pressure" with decrease in volume (Table 2). The V_2^0 is as $V_2^0{}_{Tw60} > V_2^0{}_{Tw40} > V_2^0{}_{Tw80} > V_2^0{}_{Tw20}$ is opposite to densities (Table 3). As the $V=M/\rho$ depicted a reciprocal relation between the density and V_2. Hence a stronger IMF caused higher internal pressure with higher ρ^0 and lower V_2^0. This model explained PPI. When an electron is not shifted to the other atom, a Columbic force is not generated and interaction is not possible. Here in hydrophobic the

CBF is significantly stronger, so the covalent electron is not shifted from one to another atom. When the Columbic force is zero then the AC remains integrated but in case of the HI the covalent bonded atoms have specific electronegativities with a shift of the covalent electron. It generates a columbic force for interaction. The CBF distinguished, defined and differentiated the H_bI and HI as they play an important role in each case. The CBF is shifted in one direction with a fundamental difference between the sciences of HH_bI.

3.3. Micelles formation

In water, the oxygen (O) atom has partially -2δ charge due to share electron pair shift (SEPS) of both H atoms towards O (Figure 1) and a negative charge accumulated on O and spreads as two electrons exist but the probability of finding the maximum electron density prevails on the O. It may be interacting with POES and caging around the AC to form micelles and mathematically the atomic balance is valid. But formed micelles of the Tw units are not similar to other surfactants where the hydrophilic parts are confined to the periphery while the hydrophobic is confined to a core region (Figure 2). The dark cylindrical shaped area of the Figure 2 depicts structured water forming a cage around $Tw20 = C_{11}H_{23}$, $Tw40 = C_{15}H_{33}$, $Tw60 = C_{17}H_{35}$, $Tw80 = C_7H_{14}CH=CHC_8H_{17}$ as fatty acids hydrophobic units with POES as hydrophilic unit. For example, sodium dodecyl sulfate, $-R-SO_3Na$, an anionic surfactant with $R = CH_3-CH_2-CH_2-CH_2-CH_2-CH_2-CH_2-CH_2-CH_2-CH_2-CH_2$, caused micelles. The $-OSO_3Na$ is hydrophilic and is a complementary factor to micelles as it dissociates into $R-OSO_3^- + Na^+$ where the former interacted with dipolar water. The $-OSO_3^-$ disrupted HBW for hydration sphere formation and a hydrophobic AC hangs towards the center of the spheres as a tail (Figure 2).

The bulk water did not interact but aligns around the AC and reorients towards the center of water rich spheres or hydrated $-OSO_3^-$. Thus the hydrophobically AC solvation with bulk water (HSBW) and hydrophilic POES solvation with disrupted water (HPSDW) prominently occur with Tw (Figure 2).

The HSBW is repelled to the surface by using surface energy with a weakly disrupting HBW. The Na^+ cations strongly interact and disrupt HBW and develop 1st, 2nd, and 3rd hydration spheres. The $-OSO_3^-$ hydration sphere is aligned on the outer surface and R to the center. Thus on the periphery the hydrophilic approaches to the surface to reduce the tension and the Tw are fitted in similar trends. The bulk water surround the $CH_3-CH_2-CH_2-CH_2-CH_2-CH_2-CH_2-CH_2-CH_2-CH_2-CH_2-$ with well-defined outer circular boundary. The Tw has 3 hydrophilic sites with free –OH that forms an interacting zone in continuity but AC is not dispersed in bulk water with high entropy. The H_bI developed a cage and the $-OSO_3^-$ an intensified hydrophilic zone with a distinguishable interface between philicphobic zones that developed intensified micelles where the sorbitan could be host interface (Fohel & Aswal, 2001; Gurtu, 2006; Costantino, 2000).

This mechanism of Tw is depicted in Figure 2. It represents a real science of centripetal hydrophobic AC with zigzag lines depicting the tail and centrifugal POES with darker circle depicting the head that inferred micelles formation (Figure 2). It developed different geometry and forces by reducing the γ. The hydrophobic is accumulated on the surface and the latter gets saturated. As an esterric ketonic group (C=O) adjoins the forces then it comes under strain and stress being a center of both the forces and act as an interacting driver. The O atom activity of sorbitan core group is not so effective and as a result it could not interact strongly. Thus the micelle formation is due to AC that is

Table 2. Density ($\rho \pm 10^{-3}$ kg m^{-3}), apparent molal volume ($v_2 \pm 10^{-2}$ m^3 mol^{-1}), and surface tension ($\gamma \pm 10^{-2}$ mN/m) of systems.

| M	ρ	V_2	γ	m	ρ	V_2	γ
		Tw20				Tw60	
8.44	0.999830	1035.68	59.4	8.26	0.999061	1209.91	57.22
16.87	1.000613	1084.21	57.65	16.51	1.000090	1197.9	58.68
25.28	1.002264	1064.11	55.41	24.74	1.001354	1183.01	59.86
33.67	1.003410	1068.52	54.84	32.96	1.002602	1175.1	60.31
42.04	1.004680	1067.35	54.6	41.17	1.004044	1164.57	60.78
50.39	1.006648	1051.08	54.4	49.36	1.005052	1166.24	60.45
58.73	1.007966	1050.61	54.16	57.54	1.006118	1165.91	60.52
67.05	1.009267	1050.05	53.93	65.7	1.007109	1166.5	60.96
75.35	1.012120	1026.26	52.9	73.85	1.008271	1164.06	60.65
83.63	1.012977	1033.21	52.66	81.99	1.009653	1158.74	60.35
		Tw40				Tw80	
8.42	0.999519	1128.79	62.48	8.23	0.999506	1152.95	65.48
16.83	1.000183	1166.27	61.32	16.45	1.000673	1159.25	63.81
25.22	1.001151	1165.65	60.22	24.65	1.001647	1168.26	63.45
33.61	1.002486	1153.18	59.92	32.85	1.002777	1167.04	63.1
41.97	1.003547	1151.81	59.99	41.03	1.003711	1170.69	62.74
50.33	1.004816	1145.93	60.06	49.19	1.005060	1163.6	63.66
58.67	1.005860	1145.35	59.75	57.35	1.006310	1159.81	62.5
66.99	1.006817	1145.95	58.71	65.49	1.006958	1166.6	62.54
75.3	1.007770	1146.17	58.06	73.61	1.008821	1153.32	62.25
83.6	1.009066	1141.45	57.44	81.73	1.009854	1153.54	61.91
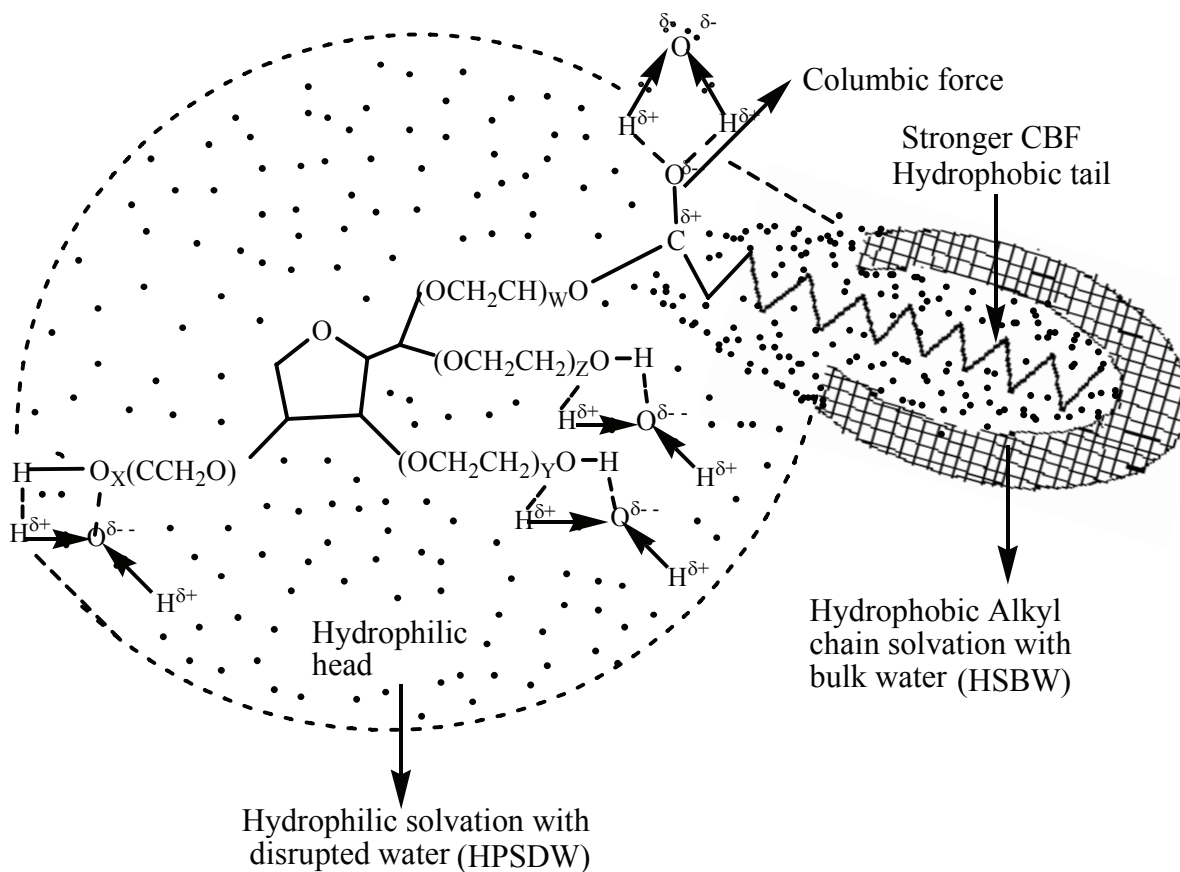
Figure 2. Tween water interaction mechanism due to unequal distribution of molecular forces at interface and equal distribution in the bulk in the context of hydrophilic and hydrophobic domains.

confined to the core as centripetal and the POES to the periphery as the centrifugal design. The dark cylindrical shaped area in Figure 2 depicts structured water forming a cage around Tw20 = $C_{11}H_{23}$, Tw40 = $C_{15}H_{33}$, Tw60 = $C_{17}H_{35}$, and Tw80 = $C_7H_{14}CH=CHC_8H_{17}$ as fatty acids hydrophobic units with POES as hydrophilic unit depicted in Figure 2.

3.4. Surface Tension (γ, mN/m)

The $\gamma_{H2O} > \gamma_{Tw60} > \gamma_{Tw20} > \gamma_{Tw80} > \gamma_{Tw40}$ with lower values by 12 mN/m as compared to water (Table 1) inferred Tw as effective surfactants. Electrostatic charges (Figure 1) on water are confined in a very small area as compared to Tw where the charges are spread along philicphobic parts. The equal charges may also be intensified but with Tw20 the hydrophilic dominates over hydrophobic and in counteraction applies a lower pressure on the surface. The γ also depicted the IMF phenomenon, and the stronger IMF showed higher γ. The $\gamma_{H2O} > \gamma_{Tw60} > \gamma_{Tw20} > \gamma_{Tw80} > \gamma_{Tw40}$ inferred higher γ with water due to stronger IMF than of the Tw. The IMF is basically a CF that works between several molecular components and becomes stronger only when the similar molecules have stronger IMF but the Tw contains two parts namely the POES and fatty acids which generate electronegative group (ENG) and Columbic forces. They are responsible for the decrease in the cohesive force (CF) with lower γ values.

3.5. Limiting surface tension

The γ^0 trend as $\gamma_{water} > \gamma^0_{Tw80} > \gamma^0_{Tw40} > \gamma^0_{Tw20} > \gamma^0_{Tw60}$ inferred 18% weakening in CF with 17.37%, 14.45%, 22.68% and 10.22% decrease in γ of Tw20, Tw40, Tw60 and Tw80 respectively (Table 3). The Tw60 caused a larger decrease in CF behaving as a good surfactant with weaker

HB of H_2O and easily approached the surface. But the Tw80 with 1 DB is not able to decrease the γ as it did not approach the surface and dispersed in the bulk phase. The 1 DB split the CBF and developed intramolecular multiple force centers that weakened the H_bI and enhanced the HI. Thus the Tw60 and Tw80 had a reverse impact on surface energies behaving as surfactants and dispersants. (Wikipedia; Levin & Flores-Mena 2001; Singh 2007; Singh & Mistra2008). However the compositional effect of Tw60 is stronger, maybe due to equal aggregation of water by developing the gel while the Tw20 is weak. The γ was determined below the CMC level (Table 2).

3.6. Spring Weight Model

The γ is a thermodynamic phenomenon and deals with the surface energy. For example, water has 72.88 mN/m γ or 72.88 mJ/m² surface energy. Figure 3 is a proposed model on the basis of the γ data. In Figure 3, negative γ^0 values are taken to show a down pull and infer an effect on meniscus of the water. For example, the position of the γ_{Tw80} is away from the Tw60 by 9.08 mN/m along with the Tw20 and Tw40 depicted in Figure 3.

Figure 3 is projected as a spring weight model (SWM) due to surface energy consumption at the interface with respect to γ_{water}. The surface energy consumption model (SECM) (Figure 3) with a pull on air-liquid interface (ALI) was developed with reference to a base line on γ^0 scale. The water meniscus was considered as a reference and its γ as a scale to construct SECM and worked on HB that analyzed a pull on ALI in terms of γ^0. It predicted the HB with reference to the water (Figure 3). A sharper downwards pull of a meniscus of water is considered as larger surface

Table 3. Limiting density $\rho^0 \pm 10^{-3} kg\ m^{-3}$, 1st degree slope $s_\rho \pm 10^{-3} kg^2\ m^{-3} mol^{-1}$, $v_2^0 \pm 10^{-2} m^3 mol^{-1}$, $s_{v2} \pm 10^{-2} m^3 kg\ mol^{-2}$ and 2nd degree slope $s_{v2}' \pm 10^{-2} m^3 kg^2\ mol^{-3}$, surface tension $\gamma^0 \pm 10^{-2} mNm^{-1}$, 1st degree slope $s_\gamma \pm 10^{-2} mNkgmol^{-1} m^{-1}$, 2nd degree slope $s_\gamma \pm 10^{-2} mNkg^2 mol^{-2} m^{-1}$, chemical potential $\mu \pm 10^{-5} Jm^{-2}$, entropy $s \pm 10^{-2} Jmol^{-1} k^{-1}$ and surface excess concentration $\tau \pm 10^{-2} mol\ m^{-2}$ obtained from regression analysis.

System	Density		AMV			Surface tension		
	ρ^0	$S\rho$	V_2^0	S_{V2}	S_{V2}'	γ^0	S_γ	S_γ'
Tw20	0.99918	0.1683	1082.56	-464.42	-3944.89	60.23	-180.262	1140.22
Tw40	0.99892	0.1428	1174.91	-918.21	6703.54	62.35	-55.6326	4.76470
Tw60	0.99885	0.1529	1205.29	-1415.28	11425.24	56.35	1155.3519	-1308.94
Tw80	0.99887	0.1027	1158.05	-8554.59	-8554.59	65.44	-75.3132	436.40

Continue Table 3---------

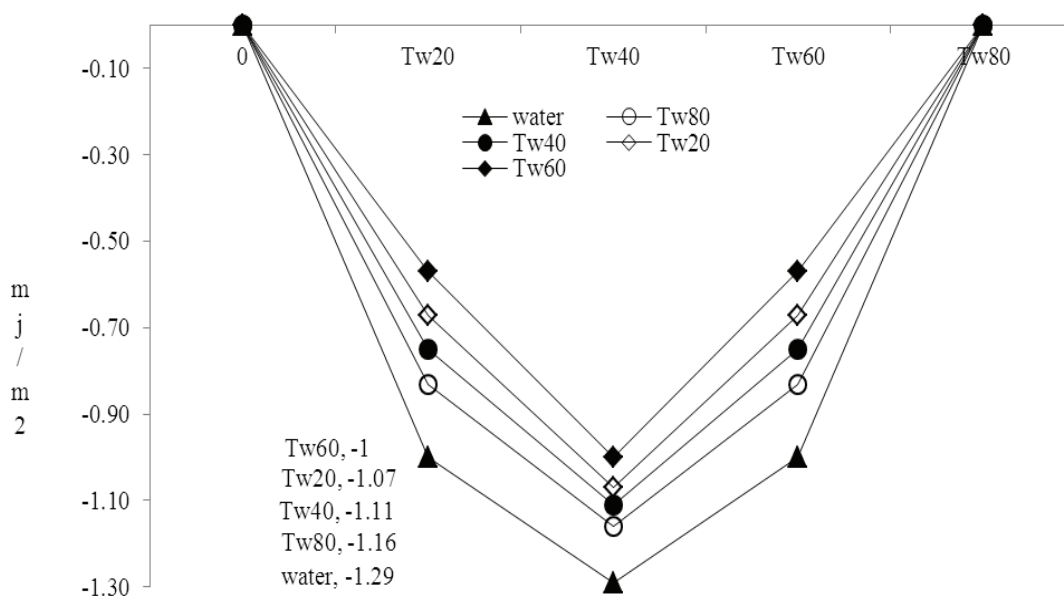| Chemical potential		Entropy	SEC
μ^S	μ^0_{Bulk}	ΔS	τ
19794.34	-12424	266.25	-0.0003
15134.69	-11944	267.20	-0.002
15371.15	-12031	266.58	-0.0018
-22197.76	-12612	267.47	0.00011

Figure 3. The surface energy consumption of the tweens with C=12, C=16, C=18, C= 18 with single double bond in context of the water surface energy as a reference. The surface energy is on the y-axis.

energy mJ/m^2 with deeper downwards pull on ALI. The SECM is a thermodynamic model as a molecular energy was used for constant pull under prescribed experimental conditions. The water with 72.88 J m^{-2} at 297.15 K is a higher surface energy liquid and the Tw weakened the pull by disrupting HB due to energy consumption (Eq. (16)) and worked against the tension that reduced γ to some extent. The Tw reduced sharpness of water curvature with substantial reduction in CF where the Tw did work in disrupting HB and in the process the CF was weakened with reduction in sharpness of the meniscus. Individually the Tw reduced meniscus in 1.29: 1.16: 1.11: 1.07: 1 ratios with water, Tw80, Tw40, Tw20 and Tw60 respectively are shown in Figure 3.

The spring-weight model is fitted in industrial applications of high surface energy liquids in simulating with several liquids. For example, pure water has weaker textile washing capacity due to stronger CF and the detergents reduced the same due to work against the tension with its energy utilization. The weaker CF inferred an energy consumption process (Figure 3) and the Tw60 showed a minimum value where both the Tw60 and Tw80 have similar AC except DB with Tw80. The latter varied a viscous flow due to inductive and steric effects. The Tw60 reduced γ by 16 mN/m. The Tw60 with a lowest surface tension has proven a stronger upwards push and weaker downwards pull with less deep meniscus pull. The Tw20 and Tw40 are with shorter AC as compared to Tw60 with higher γ than of the Tw60. With the AC, the application of steric and indicative effects was weaker in comparison to Tw60. The Tw60 acted as a good surfactant because it lowered the surface tension with a large decrease in the CF which is used widely in industry. The Tw20 and Tw40 weakly disrupted the structure. The Tw60 explained a critical role in a hydrophobic chain due to sp^3 configuration where the sp^2 and sp^3 are correlated with surface as a functional model. Eq. (17) is proposed for such simulations.

$$CF\ (SP^3, SP^2) = HBD + MR + SH + IE \qquad (17)$$

Table 4. Carbon chain ratios are depicted.

Tween	AC	XYZW	Ratio
Tw 20	12	20	0.1:01.7
Tw40	14	20	0.1:01.3
Tw60	18	20	01:01.1
Tw80	18	20	01:01.1

The CF cohesive force, HBD hydrogen bonding disruption, MR molecular reorientations, SH steric hindrance and IE are inductive effects. The ratio of philicphobic is found operational due to the molecular geometry where the philicphobic domains monitor surface energy with rationalization which is operational with Tw80 and Tw60 (Table 4).

Hence the hydrophobic and hydrophilic domains play an important role in NIS because the hydrophilic function due to stronger interacting affinity tries to disperse in bulk water but the hydrophobic AC with zero water interacting affinity tries to keep them away (Figure 4). The water molecules do not accumulate in bulk due to a networking of hydrophobic chain. Since air-water surface area is extremely accessible for hydrophobic AC, the micelles moved towards the surface and accumulated which was used to maintain the meniscus. Now it is diverted to the accumulated hydrophobic part where work is done in the process of accumulation of the hydrophobic chain. So the γ is reduced and a boundary defining the tension is diminished by weakening the CF with higher spreading power (Figure 4).

Figure 4 depicts a real micelle formation mechanism with a hydrophobic part accumulated at the surface and a hydrophilic part hanging towards the bulk phase. Notably a balancing force seems to be operational around a common point where the hydrophilic head tended downwards and a hydrophobic tail upwards due to disrupted and structured HB respectively. The abovementioned science found relevance of excess surface tension (γ^{excess}, mNm^{-1}), surface excess concentration (τ, m^2 mol^{-1}) and area per molecule (a, mol m^{-2}) in the context of reducing a pull of meniscus supported by the γ as surface energy in mJ m^{-2}. The $\gamma^{excess} = \gamma_{water} - \gamma^0_{Tw}$ was calculated and noted that it is completely the reverse of the γ^0 values. Notably the γ^{excess} is $\gamma^{excess}_{Tw60} > \gamma^{excess}_{Tw20} > \gamma^{excess}_{Tw40} > \gamma^{excess}_{Tw80}$ (Figure 5) with a maximum value of the Tw60

inferred it as an excellent surfactant for industrial purposes. The Tw60 substantially decreased the CF with lower γ data.

The γ^{excess} inferred that the higher γ^{excess} is more useful in industry as it weakened the CF. The τ denoted an excess of solute concentration per unit area of a surface as mol/m^2 with bidirectional interface with trend as $\tau_{Tw80} > \tau_{Tw20} > \tau_{Tw60} > \tau_{Tw40}$ (Figure 6).

It is inferred that the hydrophilic columbic forces are operational with Tw while the hydrophobic controlled the molecular area. The trend of τ is satisfied because in Tw80 and Tw20 stronger Columbic force work due to IMMFT (intramolecular multiple force theory) which do not allow the hydrophilic POES part to move to the surface due to stronger interaction with water and the hydrophobic part easily approaches the surface. The accumulation of Tw80 at the interface is higher because it has 18C with stronger CBF but due to 1 DB a hydrophobic character is weakened due to a shift from sp^3 to sp^2 hybridization. The π bond weakened the CBF and correspondingly strengthened the hydrophilic character in Tw 80. Thereby a larger Tw80 amount is dispersed in the bulk phase and a hydrophobic part approached at the surface. The Tw40 and Tw60 in larger amounts are being confined to the bulk where a stronger CBF with the Tw60 and weaker with the Tw40 are developed. This difference in their CBF is noted due to larger Tw60 accumulation than of the Tw40. Thus with the Tw40 the CBF is comparatively weaker than the stronger hydrophobic Tw60. The Tw60 weakened the Columbic force and strengthened the H$_b$I that inhibited their accumulation at the interface and tends to move to bulk phase. Thus the Tw80 is in a larger amount per unit area than of the others according to the trend of area per molecule as $a_{Tw80} > a_{Tw40} > a_{Tw60} > a_{Tw20}$. The area per molecule of Tw60 (a_{Tw60}) at the surface is lower in comparison to the Tw80 and Tw40. The larger numbers of molecules interact and accumulate on the surface with larger amount (Figure 6). The surface area trends may not be the same like that of τ. Figure 6 found that both the τ and 'a' should be reciprocal to each other as $\tau = 1/$'a' but many factors such as optimizations, molecular geometry in specific area and micelle-micelle repulsion and attraction play important roles. The τ and 'a' of the Tw80 are related to each other and a larger accumulation utilized a higher energy at the surface. The Tw activities in the bulk and at the interface are explained by chemical potential (μ).

Micelle formation mechanism is depicted theoretically

Fatty acid and POES developed interacting potential gradient as driving force optimised in a form of sphere with two different structural components of the water: micellel formation mechansim
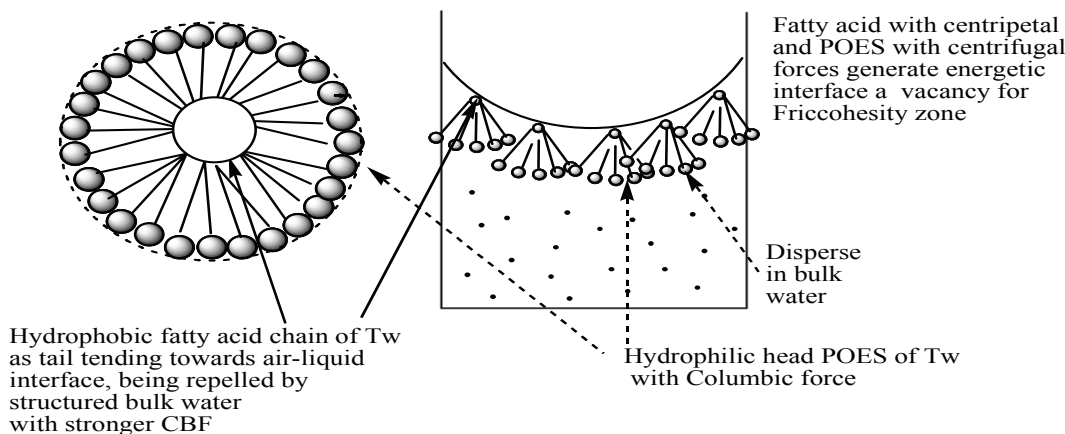

Fatty acid with centripetal and POES with centrifugal forces generate energetic interface a vacancy for Friccohesity zone

Disperse in bulk water

Hydrophobic fatty acid chain of Tw as tail tending towards air-liquid interface, being repelled by structured bulk water with stronger CBF

Hydrophilic head POES of Tw with Columbic force

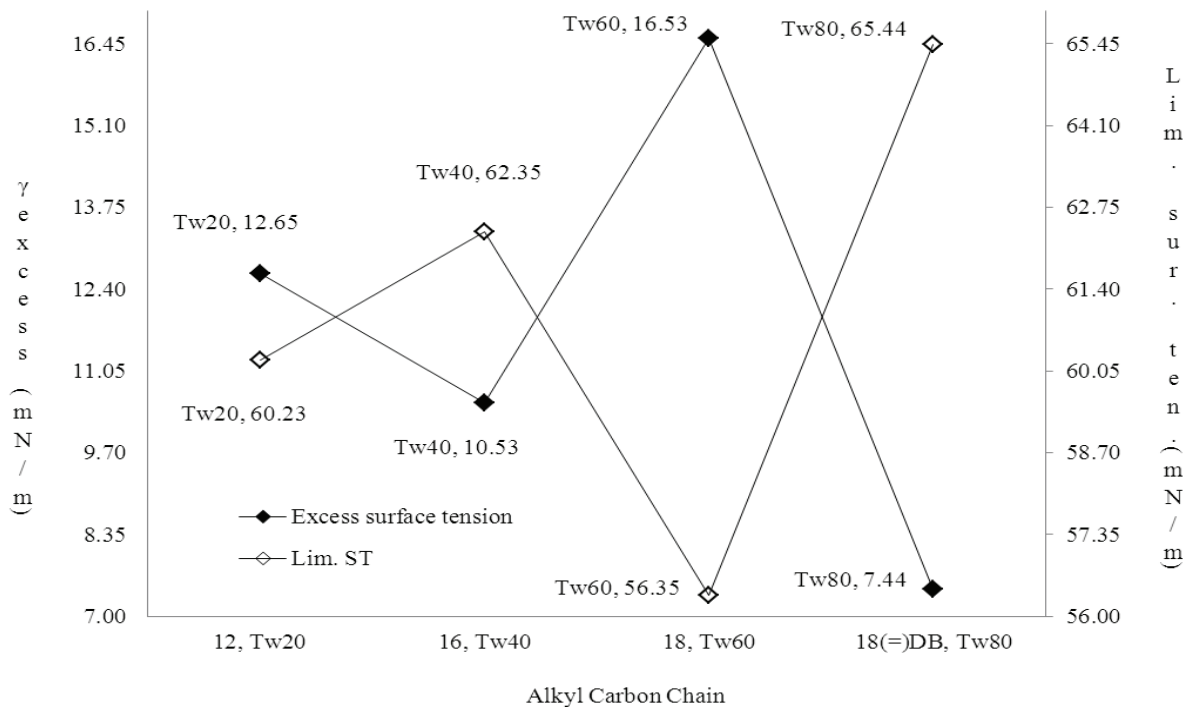*Figure 4. Surfactant Action of the Tweens at air-liquid interface.*

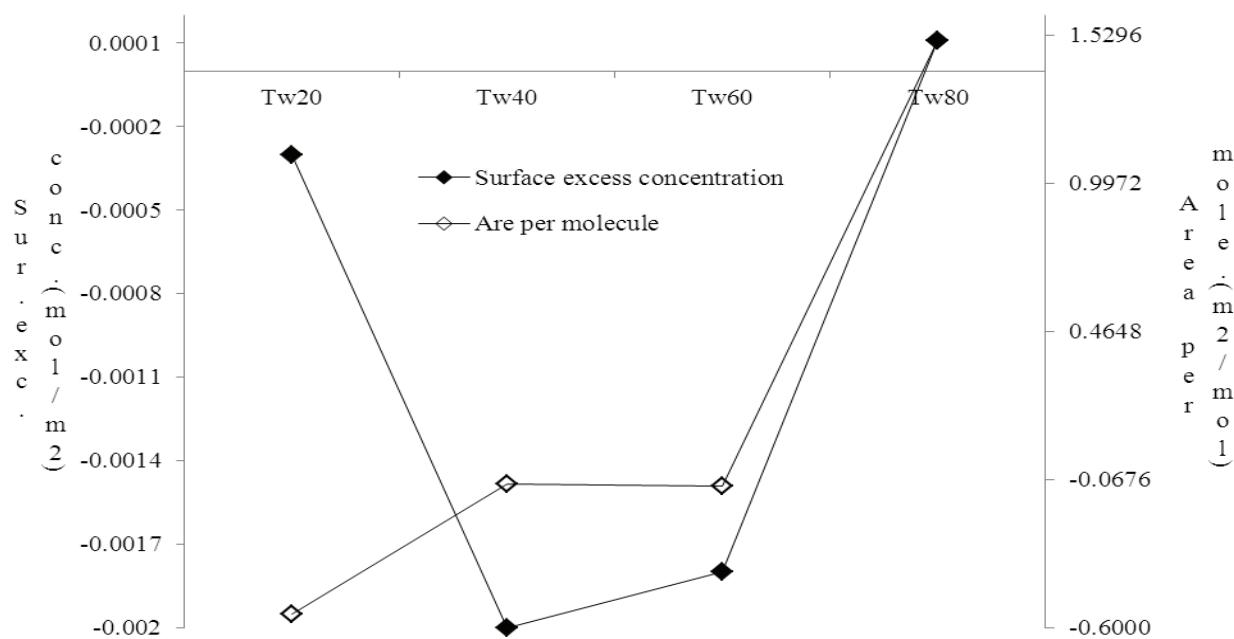*Figure 5. Limiting surface tension (mN/m) and excess surface tension (mN/m).*

Figure 6. Surface Excess concentration (τ, mol m^{-2}) and area per molecule (m^{2}mol^{-1}) at surface.

3.7. Chemical potential and Entropy

Dissimilar Tw molecules in terms of compositions developed structural reorientations accompanied by certain energy change and more importantly their HH_bI induced molecular activities at the surface and in the bulk phases respectively. Both the reorientation and activities generated entropy (ΔS, J mol^{-1}K^{-1}) and chemical potential ($\Delta \mu = \partial G/\partial n_i$, i=Tw, J mol^{-2}K^{-1})) changes respectively. The $\Delta \mu < 0 > \Delta S$ and $\Delta \mu > 0 > \Delta S$ thermodynamic states were noted in the bulk and surface phases respectively due to HB disruptive interaction and cage alignment of HBW respectively. The μ^S is as $\mu^S_{Tw20} > \mu^S_{Tw60} > \mu^S_{Tw40} > \mu^S_{Tw80}$ (Table 3), with negative μ^S for Tw80 due to disruption but with others non-disruption of the HBW at the surface. In general, the Tw60 with stronger surface activity accumulates at the surface in a larger amount resulting in

lower γ and showed $+\mu^S$. As no HB disruption occurs at the surface, a purely mechanical and weakly physicochemical phenomenon seems operational that align the structured water in a form of a cage. Due to stronger H_bI, the Tw60 moved towards the surface nearing a non-ideal system whereby both the components individually have $+ve$ μ. On mixing of non-interacting molecules together a two phase system is formed with 100% positive chemical potential as no one has utilized μ due to the ideal condition. Though such a situation is not reached in case of the Tw60 as its POES units developed weaker HI (Figure 2) but still a partial $+ve$ μ^S inferred a sizeable amount accumulated at the surface. The $\mu^S_{Tw20} > \mu^S_{Tw60}$ inferred a comparatively higher work done with stronger reorientation or alignment of structured water in forming a cage of larger size with Tw60 than of the Tw20. Though in cage alignment, a maximum

non-disruptive work is done as compared to disruptive in bulk phase as the $\mu^S > 0 > \mu^B$ thermodynamic states are noted in the study (Table 3). The $\mu^S > 0$ depicts a nonspontaneous while the $0 > \mu^B$ a spontaneous processes. Thus an integrated cage formation for a longer AC of the Tw60 occurred comparatively in larger areas with fewer multiple alignments as compared to the Tw20 at a cost of higher surface energy. It utilized comparatively a lower μ^S than of the Tw20 due to smaller sized cage with multiple alignments that utilized lower energy at the surface. Also the μ^S and μ^B data with the Tw40 inferred a competition between the POES and AC where neither a pulling down nor a pushing up occurs but a balancing of the forces by consuming higher energy than the Tw80 was noted. The two types of attraction forces are operational at the surface, namely the air liquid at upwards and the liquid-liquid forces downwards. The negative μ^S with Tw80 has marked a spontaneous process even though it should have been non-spontaneous but it is noticed that the 1 DB with Tw80 has differentiated its behavior by causing a slightly different interacting mechanism and increasing some of the hydrophilic character of the AC. The μ^B are negative with the Tw inferred that the hydrophilic part with water loving nature in bulk disrupts the HBW. The μ^B as $\mu^B_{Tw40} > \mu^B_{Tw60} > \mu^B_{Tw20} > \mu^B_{Tw80}$ inferred that the μ^B_{Tw40} value is higher because the upwards air liquid forces and the downwards liquid-liquid forces are the same but in opposite directions. Thus through these two ways the energy consumption process occurs with slightly non spontaneous due to hydrophobicity at the surface. So the cage formation and HB disruption ratio are the same and the hydrophilic part is not fully interacted with lower energy utilization.

In Tw60 the AC forms only a single cage per molecule and a hydrophilic part is easily reoriented in the bulk with higher μ energy utilization. With Tw20 the HI dominate over the H_bI and a hydrophilic part required higher energy to disrupt the HBW. The Tw80 utilized higher energy due to 1 DB in AC increased the hydrophilic character. On the basis of the μ^S and μ^B data reflection and analysis, the MPK (Mansingh Patel Kale) wave model is proposed. The MPK initials are driven from author's initials. The mechanism of the philicphobic parts is depicted in Figure 7 in a very simple and scientific manner.

The MPK wave model is also supported by entropic changes (ΔS). The ΔS as $\Delta S_{TW80} > \Delta S_{TW40} > \Delta S_{TW60} > \Delta S_{TW20}$, inferred that the Tw80 showed a higher entropy that marked a higher disorder as it developed a stronger disruption in bulk with much randomness. As per IMMFT model the π-conjugation punctured uniformity of the CBF due to sp^2 hybridization inserted in sp^3 AC. Thus the Tw80 generated the hydrophilic (POES), pseudo hydrophilic (1 DB) and hydrophobic (AC) forces where the three types of forces with higher entropic changes work. Similarly the tentropic changes may also influence the MPK model because the 1 DB causes branching motions where in a manner of tentacles the tentropic do exist and turn the interacting effects of supramolecules such as Tw80. The Tw40 generated the same forces at air liquid and the liquid-liquid forces downwards in opposite direction. The system works under an influence of both the forces without domination of either force. Both the CBF and ENG forces also work in Tw60 and Tw20 as $\Delta S_{TW60} > \Delta S_{TW20}$ where the Tw60 the CBF is dominated over ENG with many reorientation changes during the cage formation. It caused a slightly higher disorder in comparison to the Tw20 due to the water repelling nature of AC. While in Tw20 the ENG is higher in comparison to CBF and the ENG easily interacts with HBW without any difficulty and become an ordered system in comparison to the other.
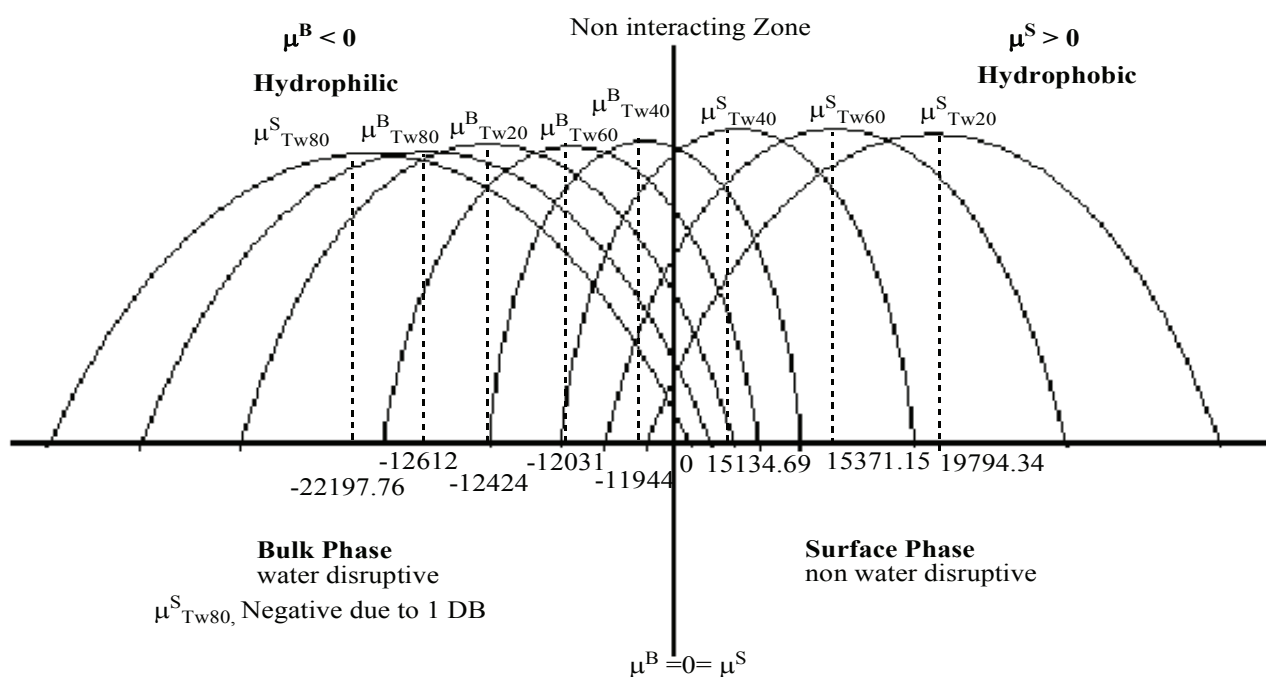

Figure 7. Thermodynamic depictation of competition between μ^S and μ^B through proposed MPK- wave model (Mansingh-Patel-Kale- wave model).

4. Conclusion

The ρ and γ data of Tw have elucidated an interacting profile and a shift from hydrophilic to hydrophobic interactions to sort out a suitable Tw member to be used industrially with higher spreading capability and a lower CF. The $\gamma^0_{Tw80} > \gamma^0_{Tw40} > \gamma^0_{Tw20} > \gamma^0_{Tw60}$ inferred decrease with a CF by 12 mN/m in Tw. It found higher decrease in Tw60 as efficient NIS. The sizes of AC and DB have influenced operational dynamics. A gel formation was noted with Tw60 but not with Tw80 due to 1 DB. It could be industrially useful for preparing gel. The DB is seen to be a most competent constitutional parameter to alter the interacting activities. The equally distributed -(-O-CH_2CH_2)-OH had equally contributed, however with the C numbers in AC influenced interacting activity by contributing to a shift from PPI. A relationship between their sizes and physicochemical properties could design a unique mixed solvents, may be useful as green chemistry with high biocompatibility for cosmetics, textiles, and blending dyeing processes. Their physicochemical profile could infer wider applications and an indicator to sensitize the HI. Thereby, any member of Tw could be an excellent biosensor as a Tw is highly biocompatible in nature with increasing AC.

Nomenclature

AC	Alkyl Chain
ALI	Air Liquid Interface
CBF	Covalent Bonding Force
CF	Cohesive Force
DB	Double Bond
HB	Hydrogen Bond
HBW	Hydrogen Bonded Water
HPSDW	Hydrophilic POES Solvation with Disrupted Water
HSBW	Hydrophobic Solvation with Bulk Water
ID	Interacting Dynamics
IMF	Inter Molecular Force
MA	Molecular Activities
MCF	Molecular Constitutional Force Model
NIS	Non-Ionic Surfactant
PCI	Physicochemical Indicators
PEG	Polyethylene Glycol
POES	Polyoxyethylene Sorbitan
PPI	Philicphobic Interacting
PWI	Pair Wise Interaction
SECM	Surface Energy Consumption
Tw	Tween
V2	Apparent Molal Volume
w/w	Weight by Weight

Greek letters

ΔS	Entropic change
a	Molecular area
γ	Surface Tension
γ^{excess}	Excess surface tension
μ^B	Bulk chemical potential
μ^S	Surface chemical potential
ρ	Density
τ	Surface excess concentration

References

Bakshi, Kaur, M. S., Kaur, A. (2006). Effect of temperature on the unfavorable mixing between tetraethylene glycol dodecyl ether and plusomic. *G. J. Colloidal Interface Sci.* 1, 296-370.

Bartschat, K. (1992). Mitt Scattering and angular momentum orientation low-energy electron Scattering from indium atom. *J. Phys. B. At Mol. Opt. Phys,* 25, L307.

Costantino, L., Errico, G. D., Roscigno, P., and Vitagliano, V. (2000). Effect of Urea and Alkylureas on Micelle Formation by Non-ionic surfactant with Short Hydrophobic Tail at 25.0^{0}C. *J. Phys. Chem.* B104, 7326-7333.

Denial, R. S., Woodrow L. S., Daniel P. L. (2003). Lorenz force effect in magneto turbulence. *Elsevie Science direct, Physics of the earth and planetary Interior,* 135, 137-159.

Dubost, H. (1998). Picosecond to Minute Molecular Vibrational Dynamics in Crystosolids. *J. of low temp. phys.* 111, 615-628.

Elliott, R. S., Shaw, J. A. Triantafyllidis, N. (2006). Stability of crystalline solids-II: Application to temperature-induced martensitic phase transformations in a bi-atomic crystal. *J. Mech. Phys. Solids*, 54, 193-232.

Fohel, P.S., Aswal, V.K. (2001). Miceller structure inter-micelle interaction in miceller solutions: Results of small angle neutron scattering studies. *Current science*, 80, 8-2.

Gurtu, J. N. (2006). Advance Physical Chemistry. *Eight Revised Edition,* 592-600.

Hafner, J. (2003). Vibrational spectroscopy using AB initio density-functional techniques. *J. Mol. Struct*, 3, 651-653.

JianBin, Z., GpengYan, Z., Kai, M., Fung, H., GuoHua, C., XiongHui, W. (2008). Hydrogen bonding interactions between ethylene glycol and water: density, excess molar volume, and spectral study. *Sci. China. Series B: Chem*, 51, 420-426.

Kao, M. J., Tien, D. C., Jwo, C. S. and Tsung, T. T. (2005). The study of hydrophilic characteristic of ethylene glycol. *J. of physics*, 13, 442-445.

Kohler, M., Lunkenheimer, P., and Loide, A. (2008). Dielectric and conductivity relaxation in mixture of glycerol with LiCl. *Eur. Phys. J. E. Soft Matter*, 27(2), 114-122.

Lee, Dal-Heui., Kim, Eun-Sik., Chang, Ho-Wan. (2005). Effect of Tween surfactant compounds for remediation of toluene- contaminated groundwater. *Geosciences J.* 9(3), 261-267.

Levin, Y., and Flores-Mena, J. E. (2001). Surface tension of strong electrolytes solution. *Euro physics. Lett.* 56(2), 187-192.

Mitropoulos, A. Ch. (2008). What is surface excess? 1, 1-3.

Rossnagel, K., Smith, N. V. (2006). Spin-orbit coupling in the band structure of reconstructed 1T-TaS$_2$. *Phys. Rev. B*. 73, 073106.

Singh, A., Mistra, V. K., Patel, S.K., Sheikh, S., Sadhu K. and Courey N. K. (2010a). Effect of surfactant on Two immiscible liquid by Mansingh Survismeter. *Int. J. of Pharmacy and Life sciences*, 1(3), 182-187.

Singh, M. (2005). A Simple Instrument for Measuring the Surface Tension And Viscosity of Liquids. *J. Instrum. Exp. Technol*. 48, 270-271.

Singh, M. (2006a). Experimentally for hydrophilic and hydrophobic interactions analysis of N methyl ureas with water using density and surface tension. *J. Biochem. Biophy. Methods*, 67, 151-161.

Singh, M. (2006b). Survismeter- Type I and II for surface tension, Viscosity measurement of liquids for academic, and research development studies. *J. Biochem. Biophy. Methods*, 67(30), 151-161.

Singh, M. (2007). Survismeter 2-in-1 for viscosity and surface tension measurement, an excellent invention for industrial proliferation of surface forces in liquid. *Surface Review and Letters*, 14 (05), 973-983.

Singh, M. (2008). Pre-requisite physico-chemical studies of 1,3,5 triazine for micro mixing with wax emulsion + 4-nonyl phenol ethoxylate, estimated with SEM technique. *Phys. Chem. Liq*. 46, 98-110.

Singh, M., Kumar, A. (2006). Hydrophobic interaction of Methylureas in Aqueous Solutions Estimated with Density, Molal Volume, Viscosity and Surface Tension from 293.15 to 303.15K. *J. of Sol. Chem*. 35(4).

Singh, M., Matsuoka, H. (2009) Liquid-liquid interface study of hydrocarbons, alcohols, and cationic surfactants with water. *Surface Review and Latters*, 16(4), 599-608.

Singh, M., Mistra V. K. (2008). Solvodynemics of Benzene and water phases by DTAB, MTOAC, TMSOL and Orcinol studied with Interfacial Tension, Surface Tension and Viscosity measured with Survismeter. *Int. J. of Thermo*. 11, 181-186.

Singh, M., Mistra, V. K., Kale, R.K., Jain, C. L. (2010b). Molecular Activation Energies ($\Delta\mu_2^*$) OF L-Lusine, L-Tyrosine,DL-Alanine,Glycerol,Orcinol,Iodine,DTAB, and TMSOI for blending with Melamine-Formaldehyde-Polyvinylpyrrolidone Polymer Resin Illustrated with SEM. *J. App. Polym. Sci.*

Singh, M., Sharma, Y. K. (2006b). Activation Energy and Transition State Theory Applications for Interactions of Nucleos (t)ides and Furanose Puckering in Aqueous Medium from 288.15 to 298.15 K. *Phys. Chem. Liq.*, 1, 44.

Singh, M., Sharma, Y. K. (2006a). Volumetric and viscometer studied of Nucleosides, Nucleotides and Sugar in Aqueous Medium from 288.15 to 298.15K. *Iran J. Chem. Eng.* 25(1), 53-66.

Singh, M., Sushma, (2009). Studies of densities, apparent Molar volume , viscosities, surface tension and free energies of activation for interactions of praseodynemiumsalzen complex with dimethylsulphoxide. *J. Mol.Liq.* 148, 6-12.

Surface tension of water vs temperature. Wikipedia. Org./wiki/properties of water.

Valery, C., Pouget, E., Pandit, A., Verbavatz, J. M., Bordes, L., Boisde, I., Cherif-Cheikh, R., Artzne, F., Paternostre, M. (2008). Molecular origin of the self-Assembly of Lanreotide into Nanotubes: A Mutational Approach. *Biophys. J.* 94, 1782-1795.

Wendlandt, J. (2005). Study of with hydrogen binding in small water cluers with density functional theory calculation.